ChemPubSoc Europe

DOI: 10.1002/chem.201402358

CHEMISTRY A European Journal Full Paper

Zwitterions

C_{sp^3}—H Bond Activation with Triel Metals: Indium and Gallium Zwitterions through Internal Hydride Abstraction in Rigid Salan Ligands**

Nicolas Maudoux,[a] Jian Fang,[b] Thierry Roisnel,[c] Vincent Dorcet,[c] Laurent Maron,[b] Jean-François Carpentier,*[a] and Yann Sarazin*[a]

Abstract: The hydropyrimidine salan (salan = *N*,*N*′-dimethyl-*N*,*N*′-bis[(2-hydroxyphenyl)methylene]-1,2-diaminoethane) proteo-ligands with a rigid backbone {ON^(CH_2)^NO}H_2 react with $M(CH_2SiMe_3)_3$ (M = Ga, In) to yield the zwitterions {ON^(CH^+)^NO}$M^-(CH_2SiMe_3)_2$ (M = Ga, **2**; In, **3**) by abstraction of a hydride from the ligand backbone followed by elimination of dihydrogen. By contrast, with Al_2Me_6, the neutral-at-metal bimetallic complex [{ON^(CH_2)^NO}AlMe]$_2$ (**[1]$_2$**) is obtained quantitatively. The formation of indium zwitterions is also observed with sterically more encumbered ligands containing *o*-Me substituents on the phenolic rings, or an N(CHPh)N moiety in the heterocyclic core. Overall, the ease of C_{sp^3}—H bond activation follows the order Al ≪ Ga < In. Experimental data based on model complexes, XRD studies, and ^{2}H NMR spectroscopy show that the formation of the Ga/In zwitterion involves rapid release of $SiMe_4$ followed by evolution of H_2, and suggest the formation of a transient metal-hydride species. DFT calculations indicate that the systems {ON^(CH_2)^NO}H_2 + $M(CH_2SiMe_3)_3$ (M = Al, Ga, In) all initially lead to the formation of the neutral monophenolate dihydrocarbyl species through a single protonolysis. From here, the thermodynamic product, the model neutral-at-metal complex **1**, is formed in the case of aluminum after a second protonolysis. On the other hand, lower activation energy pathways lead to the generation of zwitterionic complexes **2** and **3** in the cases of gallium and indium, and the formation of these zwitterions obeys a strict kinetic control; the computations suggest that, as inferred from the experimental data, the reaction proceeds through an instable metal-hydride species, which could not be isolated synthetically.

Introduction

The activation of α-amino C_{sp^3}—H bonds, notably by α-lithiation and transition-metal-catalyzed activations in which an N-heterocycle participates as the nucleophilic coupling partner, affords convenient access to nitrogen-containing building blocks.[1] The α-alkylation of $HNMe_2$ with alkenes catalyzed by $M(NMe_2)_x$ (M = Zr, Nb, Ta; x = 4,5) was reported in the 1980s,[2] and the hydroaminoalkylation catalyzed by d^0 complexes of group 4–5 metals is now a key reaction.[3,4] Late transition metal catalysts are also known to activate the α-amino C_{sp^3}—H bond,[5] but examples of α-C–H addition of alkylamines to alkenes mediated by main-group metals are seldom. The activation of α-amino C_{sp^3}—H bonds leads to the formation of byproducts during the hydroamination of vinylarenes catalyzed by alkali amides,[6] but similar reactivity is not reported for group 13 metals: aluminum, gallium, and indium (referred to as triel metals).

β-Hydride elimination has long been known to be a key process in organometallic chemistry, including for Al and related triel elements.[7] Hydrogen transfer from the α position of nitrogen in 2-substituted indoline derivatives has been used to reduce imines in metal-free transfer hydrogenation reactions.[8,9] Uhl and co-workers have reported a unique case of C_{sp^2}—H bond activation upon treatment of di(*tert*-butyl)butadiyne with AlR_2H (R = Me, *t*Bu).[10] However, we are not aware of intramolecular abstraction of hydride from α-amino C_{sp^3}—H moieties (an umpolung vis-à-vis the above examples of α-amino C_{sp^3}—H bond activations) and concomitant generation of

[a] *N. Maudoux, Prof. Dr. J.-F. Carpentier, Dr. Y. Sarazin*
Organometallics: Materials and Catalysis Department
Institut des Sciences Chimiques de Rennes
UMR 6226 CNRS—Université de Rennes 1
Campus de Beaulieu, 35042 Rennes (France)
E-mail: jean-francois.carpentier@univ-rennes1.fr
yann.sarazin@univ-rennes1.fr

[b] *Dr. J. Fang, Prof. Dr. L. Maron*
Laboratoire de Physique et Chimie de Nano-objets
UMR 5215 CNRS—Université de Toulouse
135 avenue de Rangueil, 31077 Toulouse (France)

[c] *Dr. T. Roisnel, Dr. V. Dorcet*
Centre de Diffractométrie des Rayons X
Institut des Sciences Chimiques de Rennes
UMR 6226 CNRS—Université de Rennes 1
35042 Rennes (France)

[**] *Salan* = N,N′-*dimethyl*-N,N′-*bis[(2-hydroxyphenyl)methylene]-1,2-diaminoethane.*

Supporting information for this article is available on the WWW under http://dx.doi.org/10.1002/chem.201402358.

stable carbocations mediated by triel metals, which act as hydride acceptors.

Herein, we report such an example and highlight the role of the triel metal when metal hydrocarbyls are reacted with rigid hydropyrimidine-bridged salan proteo-ligands, with effective C_{sp^3}—H activation mediated by gallium and indium but not by aluminum. Experimental data combined with DFT computations demonstrate that the larger triel atoms act as hydride acceptors to eventually release dihydrogen, and that the formation of zwitterions with gallium and indium is dictated by a kinetic regime.

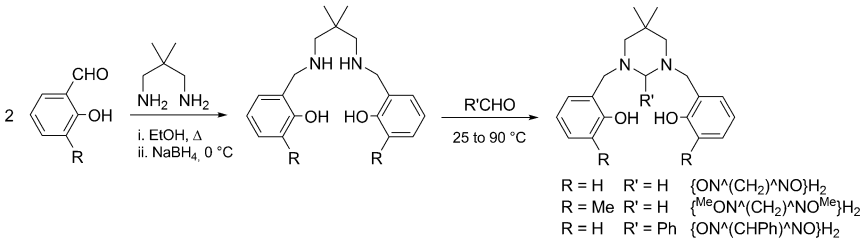

Scheme 1. Preparation of the salan proteo-ligand $\{ON\text{^}(CH_2)\text{^}NO\}H_2$ and the substituted analogues $\{^{Me}ON\text{^}(CH_2)\text{^}NO^{Me}\}H_2$ and $\{ON\text{^}(CHPh)\text{^}NO\}H_2$.

Results and Discussion

Experimental studies

The new salan proteo-ligand $\{ON\text{^}(CH_2)\text{^}NO\}H_2$ rigidified by a hydropyrimidine core was prepared straightforwardly in 75% yield by the Mannich reaction between salicylaldehyde and 2,2-dimethyl-1,3-diaminopropane. The substituted analogues $\{^{Me}ON\text{^}(CH_2)\text{^}NO^{Me}\}H_2$ and $\{ON\text{^}(CHPh)\text{^}NO\}H_2$ were prepared similarly in 81 and 90% yields, respectively, starting from the corresponding salicylaldehyde and diamines (Scheme 1).

The stoichiometric reaction of $\{ON\text{^}(CH_2)\text{^}NO\}H_2$ with Al_2Me_6 at 70 °C yields $[\{ON\text{^}(CH_2)\text{^}NO\}AlMe]_2$ (**[1]$_2$**; Scheme 2); the production of this bimetallic complex is not unexpected in view of recent reports on related bis(phenolate) aluminum complexes.[11] By contrast, the reactions with $M(CH_2SiMe_3)_3$ (M = Ga, In) based on the larger (r_{ionic}: Al^{3+}, 0.32 Å; Ga^{3+}, 0.47 Å; In^{3+}, 0.62 Å) metals neatly afford the monometallic zwitterions $\{ON\text{^}(CH^+)\text{^}NO\}M^-(CH_2SiMe_3)_2$ (M = Ga, **2**; In, **3**) through abstraction of a hydride from the ligand backbone and elimination of dihydrogen (experimentally detected, see below; Scheme 3). These air-stable zwitterions feature both a carbocation stabilized by two adjacent nitrogen atoms and a formal negative charge located on the metal center. To our knowledge, such Ga-/In-mediated intramolecular C_{sp^3}—H activation is not documented.[12,13] Beyond sheer acid–base Lewis adducts, heavier triel (Ga, In) zwitterions can form through bimolecular addition processes,[14] but intramolecular activation is limited to the use of phosphine–gallanes and –indanes for the formation of M^-–Au^{I+} species (M = Ga, In) following chloride transfer from gold to the triel metal.[15] We have verified that the treatment of $Al(CH_2SiMe_3)_3$ (instead of Al_2Me_6) with $\{ON\text{^}(CH_2)\text{^}NO\}H_2$ equally failed to return zwitterionic complexes.

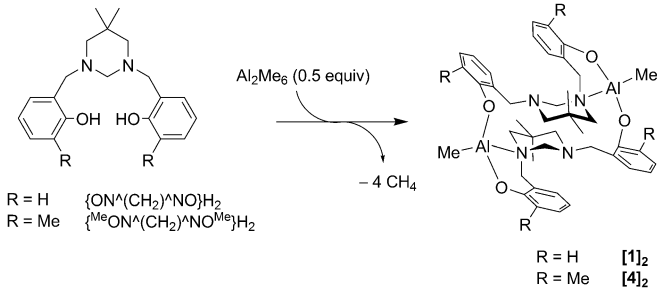

Scheme 2. Synthesis of neutral aluminum complexes.

These observations apply to some extent to sterically more congested ligands and/or when the hydride-donating capability is modified. The addition of *ortho*-Me groups on the phenolic rings (as in $\{^{Me}ON\text{^}(CH_2)\text{^}NO^{Me}\}H_2$) or the introduction of a 2-Ph group in the heterocyclic fragment (as in $\{ON\text{^}(CHPh)\text{^}NO\}H_2$) affords rigid and bulky proteo-ligands,[16] which upon treatment with Al_2Me_6 or $In(CH_2SiMe_3)_3$ give the bimetallic Al complex **[4]$_2$** (Scheme 2) and the zwitterions $\{ON\text{^}(CPh^+)\text{^}NO\}In^-(CH_2SiMe_3)_2$ (**5**) and $\{^{Me}ON\text{^}(CH^+)\text{^}NO^{Me}\}In^-(CH_2SiMe_3)_2$ (**6**) (Scheme 3), respectively. The formation of the indium zwitterion **6** requires more forcing conditions (90 h at 90 °C) than for **3** (22 h at 70 °C) in which the ligand is less cumbersome, whereas the gallium congener of **6** cannot actually be prepared, as the reaction halts after the first protonolysis to yield $[\{^{Me}ON\text{^}(CH_2)\text{^}NO^{Me}\}H]Ga(CH_2SiMe_3)_2$ (**7-H**, see below). The formation of **5** takes place at 80 °C, that is, steric considerations are preponderant for *ortho* substituents on the phenolic moieties.[17]

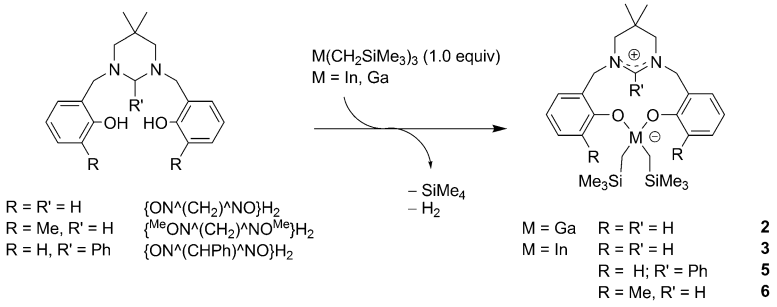

Scheme 3. Synthesis of zwitterionic gallium/indium complexes.

The complexes have been characterized by NMR spectroscopy and elemental analysis, and by X-ray diffraction crystallography in several cases. In the ^{1}H NMR spectra of the charge-neutral aluminum complexes **[1]$_2$** and **[4]$_2$** in C_6D_6, the Al–Me group is identified by a sharp singlet at high field ($\delta_{1H} = -0.33$ and -0.25 ppm, respectively). The ^{1}H NMR spectra of zwitterions **2**, **3**, and **6** exhibit a sharp, deshielded singlet at about $\delta = 7.92$–8.13 ppm characteristic of the NC*H*N$^+$ hydrogen in the carbocation. Compared with that of the proteo-ligand {ON^(CHPh)^NO}H$_2$, the solid-state FTIR spectrum of the indium complex **3** shows a new, intense absorption band at $\nu = 1674$ cm^{-1}, that is, in the region typical of the stretching frequency for C=N imine bonds; the corresponding band in the gallium analogue **2** appears at $\nu = 1682$ cm^{-1}.[16]

The molecular solid-state structures of **[1]$_2$**, **2**, **3**, and **5** have been established by X-ray diffraction crystallography. In the structure of **[1]$_2$** depicted in Figure 1, each aluminum atom is four-coordinated and lies in a tetrahedral environment through

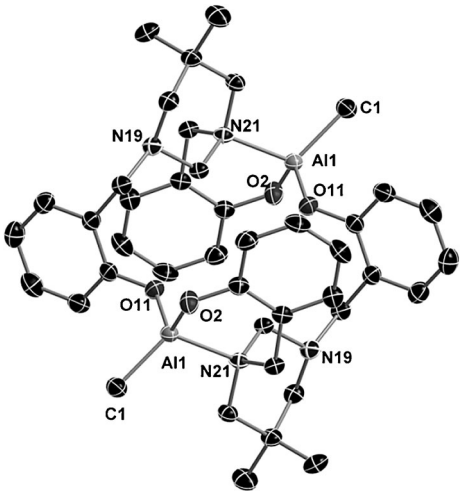

Figure 1. Molecular structure of [{ON^(CH$_2$)^NO}AlMe]$_2$ (**[1]$_2$**) in the solid state. Hydrogen atoms are omitted for clarity. Ellipsoids are drawn at the 50% probability level. Pertinent bond lengths [Å] and angles [°]: C(1)–Al(1) 1.943(2), O(2)–Al(1) 1.748(1), O(11)–Al(1) 1.734(1), N(21)–Al(1)$^{\#1}$ 2.008(1); O(11)-Al(1)-O(2) 112.63(6), O(11)-Al(1)-C(1) 115.04(7), O(2)-Al(1)-C(1) 112.69(7), O(11)-Al(1)-N(21)$^{\#1}$ 100.11(5), O(2)-Al(1)-N(21)$^{\#1}$ 100.30(5), C(1)-Al(1)-N(21)$^{\#1}$ 114.52(6); #1 = symmetry related.

coordination of two $O_{phenolate}$ and only one $N_{heterocycle}$ atoms (N(21))[18] in addition to the alkyl moiety (C(1)); this is unusual because aluminum–salen and –salan complexes are known to generally adopt five-coordinated geometries.[19] The central pyrimidine core retains the chair conformation found in the parent proteo-ligand. The bond lengths in **[1]$_2$** are unexceptional, and match those found in Gibson's Al–salan alkyl complexes featuring an *N*,*N*-disubstituted ethylenediamine bridge,[20] and those reported by Fulton for his {ONNO}AlMe complex supported by a piperazine-bridged dianionic salan ligand.[21] Each {ON^(CH$_2$)^NO}$^{2-}$ ligand in **[1]$_2$** binds to the two Al atoms through Al–$O_{phenolate}$ σ bonds. Interestingly, Fulton's complex featuring a rigid backbone (in which the piperazine adopts a boat conformation) akin to that in **[1]$_2$** is monomeric and monometallic, whereas our repeated attempts only afforded the bimetallic, dimeric **[1]$_2$**.

The gallium and indium complexes **2** and **3** are isostructural, and only the latter is presented here. In the structure of **3** (Figure 2), the four-coordinated indium atom lies in a distorted tetrahedral environment; bond lengths to the coordinated O and C atoms are not impacted by the formal negative charge

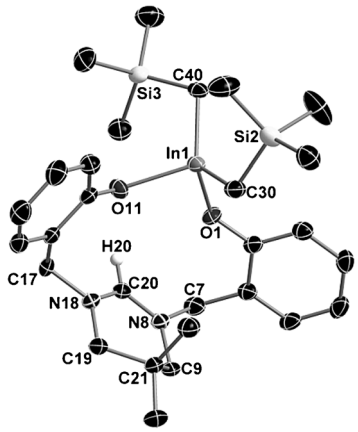

Figure 2. Molecular structure of {ON^(CH$^+$)^NO}In$^-$(CH$_2$SiMe$_3$)$_2$ (**3**) in the solid state. Hydrogen atoms and noninteracting solvent (Et$_2$O) are omitted for clarity. Ellipsoids are drawn at the 50% probability level. Pertinent bond lengths [Å] and angles [°]: In(1)–O(11) 2.110(2), In(1)–O(1) 2.116(2), In(1)–C(30) 2.167(3), In(1)–C(40) 2.171(3), N(8)–C(20) 1.323(3), N(18)–C(20) 1.304(3); N(18)-C(20)-N(8) 124.2(3), N(18)-C(20)-H(20) 117.9, N(8)-C(20)-H(20) 117.9, C(20)-N(8)-C(9) 120.5(2), C(20)-N(8)-C(7) 120.8(2), C(9)-N(8)-C(7) 118.7(2).

at the metal and fall in the expected range.[22] The unusually stable half-chair conformation of the pentahydropyrimidinium core in **3** differs from the chair conformation of the hydropyrimidine in {ON^(CH$_2$)^NO}H$_2$.[16] The C(21) atom rests 0.65 Å above the perfect plane formed by C(9), N(8), C(20), N(18), and C(19), and which also contains the C(7) and C(17) atoms. The geometries around the now sp^2-hybridized N(8), N(18), and positively charged C(20)$^+$ atoms are perfectly trigonal planar ($\Sigma_{angles} = 360°$). The C(20)–N(8) and C(20)–N(18) distances in **3** (1.32 and 1.30 Å) are much shorter than the corresponding ones in the {ON^(CH$_2$)^NO}H$_2$ (1.47 Å). They in fact come close to that for the C=N imine bond (ca. 1.28 Å), thus indicating substantial donation of the nitrogen lone pairs into the formally empty p orbital on C(20)$^+$; this is consistent with the FTIR spectrum for this complex (see above). The other bond lengths in the heterocyclic core are not affected upon formation of **3**.[23]

The structure of **5** (Figure 3) resembles that of **3**, and indeed the In–C and In–O bond lengths in the two complexes are near-identical. The impact of the phenyl substituent on the $C_{sp^2}{}^+$ carbocation on the overall geometry of the zwitterion is minimal. A smaller distance between the metal atom and the two $CH_2C(CH_3)_2CH_2$ carbon atoms at the back of the hydropyrimidine ring are measured in **5** (5.38 and 5.48 Å in **3**; 4.27 and 4.46 Å in **5**). Accordingly, the angle between the two O-In-O and C-N-C$^+$-N-C average planes is larger in **3** (78.8°) than in **5**

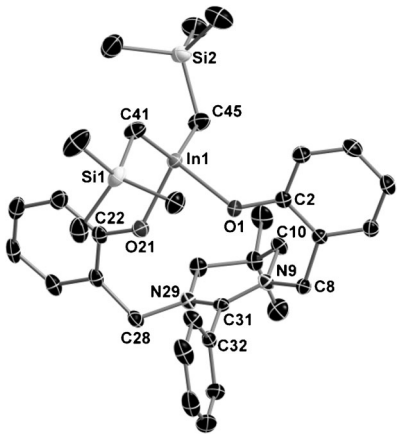

Figure 3. Molecular structure of {ON^(CPh^+)^NO}$In^-(CH_2SiMe_3)_2$ (**5**) in the solid state. Hydrogen atoms are omitted for clarity. Ellipsoids are drawn at the 50% probability level. Pertinent bond lengths [Å] and angles [°]: In(1)–O(21) 2.107(1), In(1)–O(1) 2.109(1), In(1)–C(41) 2.161(2), In(1)–C(45) 2.171(2), N(9)–C(31) 1.324(2), C(8)–N(9) 1.477(2), N(29)–C(31) 1.326(2), C(28)–N(29) 1.477(2); C(31)-N(9)-C(10) 121.20(12), C(31)-N(9)-C(8) 123.23(12), C(10)-N(9)-C(8) 115.28(11).

(57.1°), and the distance to the carbocation is greater in the latter (In···C^+ = 4.19 Å in **5** and 4.08 Å in **3**). Besides, the angle between the two mean planes defined by the phenolic rings is wide in **3** (54.7°), but it is considerably narrower in **5** (21.1°).

^{1}H NMR monitoring of the formation of **3** in C_6D_6 (70 °C) indicated quantitative release of $SiMe_4$ whereas a singlet of low intensity at δ_{1H} = 4.47 ppm was attributed to solubilized H_2.[24] The formation of large amounts of dihydrogen in the course of the reaction was further corroborated by gas chromatography analysis.[16] The monitoring by ^{1}H and ^{2}H NMR spectroscopies of the reaction of the deuterated {ON^(CH_2)^NO}D_2 (δ_{2H} = 10.19 ppm in C_6H_6; obtained by treating {ON^(CH_2)^NO}Li_2 with excess D_2O) and $In(CH_2SiMe_3)_3$ (1.0 equiv) carried out at 25 °C in C_6H_6 revealed quantitative release of Me_3SiCH_2D and formation of [{ON^(CH_2)^NO}D]$In(CH_2SiMe_3)_2$ (δ_{2H} = 9.82 ppm in C_6H_6) within the first point of analysis (Scheme 4). No further change was noted until the temperature was raised to 70 °C, when quantitative production of **3** was observed over about 8 h; the evolution of HD was not detected spectroscopically.

The scenario was identical with gallium, but for the fact that the formation of **2** was slower than that of its indium congener and required heating to 100 °C in (deuterated) THF. The reaction of the bulkier proteo-ligand {^{Me}ON^(CH_2)^NO^{Me}}H_2 with $In(CH_2SiMe_3)_3$ proceeded more slowly (in comparison with the non *o*-Me-substituted case) but still returned **6** (slightly contaminated with **9**; see below), whereas with $Ga(CH_2SiMe_3)_3$ it stopped at the formation of [{^{Me}ON^(CH_2)^NO^{Me}}H]$Ga(CH_2SiMe_3)_2$ (**7-H**). This gallium complex was fully characterized, including by XRD studies (Figure 4); it is robust and does not evolve towards zwitterionic or neutral-at-metal bis(phenolate) species even upon heating to 100 °C for 48 h. Correspondingly, the reaction of {^{Me}ON^(CH_2)^NO^{Me}}D_2 (δ_{2H} = 10.32 ppm) with $Ga(CH_2SiMe_3)_3$ (1.0 equiv) yielded [{^{Me}ON^(CH_2)^NO^{Me}}D]$Ga(CH_2SiMe_3)_2$ (**7-D**, δ_{2H} = 9.40 ppm), see Scheme 4.[25] Finally, the proteo-ligand {Me^^{Me}ON^(CH_2)^NO^{Me}}H (obtained following a seven-step synthesis)[16] gave {Me^^{Me}ON^(CH_2)^NO^{Me}}$In(CH_2SiMe_3)_2$ (**8-Me**) upon reaction with $In(CH_2SiMe_3)_3$ (1.0 equiv). This complex did not evolve further upon heating to 130–150 °C for 12–24 h, and in particular the abstraction of hydride resulting in the formation of a hydropyrimidinium moiety was not detected. Yet, formation of an indium zwitterion is thermodynamically favored with a bisphenol, as the equimolar reaction of **8-Me** with {ON^(CH_2)^NO}H_2 returned **3** through ligand exchange and release of {Me^^{Me}ON^(CH_2)^NO^{Me}}H (Scheme 4). Note that formation of a zwitterion does not occur upon mixing **8-Me** and *o*-cresol.

The solid-state structure of the monophenoxide gallium **7-H** (Figure 4) is informative. The four-coordinated metal atom rests in a near-ideal tetrahedral

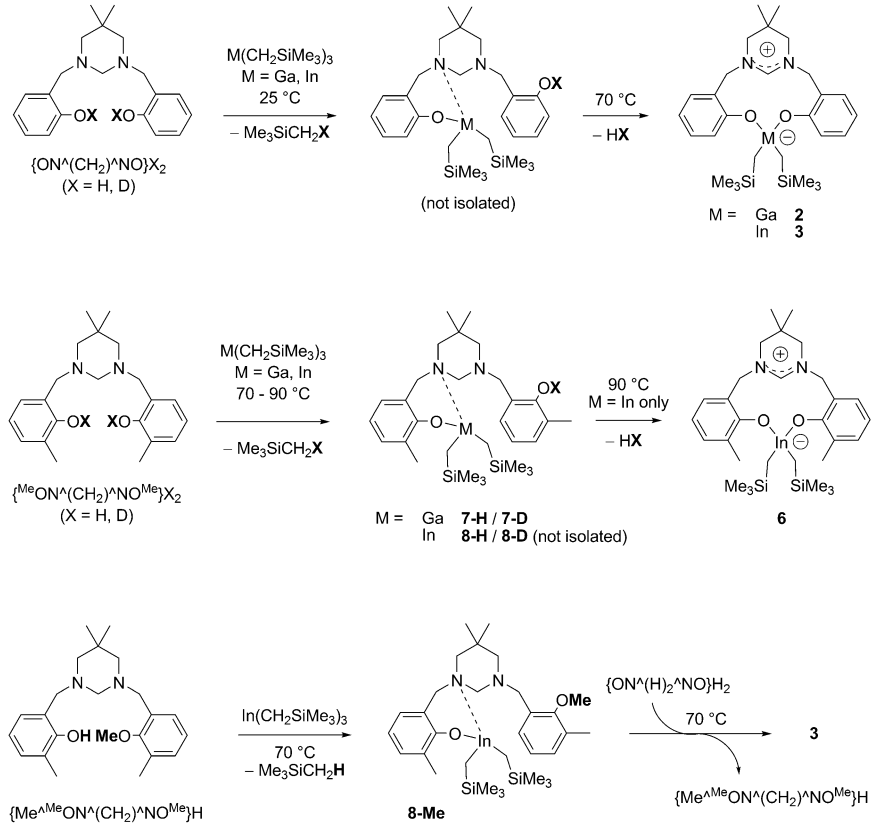

Scheme 4. Intermediates and products in the synthesis of Ga/In zwitterions.

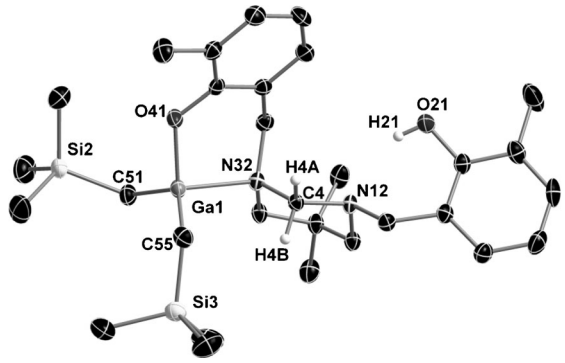

Figure 4. Molecular structure of [{^{Me}ON^(CH$_2$)^NO^{Me}}H]Ga(CH$_2$SiMe$_3$)$_2$ (**7-H**) in the solid state. Hydrogen atoms are omitted for clarity. Ellipsoids are drawn at the 50% probability level. Pertinent bond lengths [Å] and angles [°]: N(32)–Ga(1) 2.148(2), O(41)–Ga(1) 1.873(1), C(51)–Ga(1) 1.962(2), C(55)–Ga(1) 1.977(2); N(12)-C(4)-N(32) 112.5(2), N(12)-C(4)-H(4 A) 109.1, N(32)-C(4)-H(4 A) 109.1, N(12)-C(4)-H(4B) 109.1, N(32)-C(4)-H(4B) 109.1, H(4 A)-C(4)-H(4B) 107.8, C(4)-N(32)-C(31) 109.4(1), C(4)-N(32)-C(33) 112.5(2), C(31)-N(32)-C(33) 111.4(2), C(4)-N(32)-Ga(1) 108.6(1), C(31)-N(32)-Ga(1) 108.6(1), C(33)-N(32)-Ga(1) 106.1(1), O(41)-Ga(1)-C(51) 108.14(8), O(41)-Ga(1)-C(55) 107.91(8), C(51)-Ga(1)-C(55) 126.68(9), O(41)-Ga(1)-N(32) 95.05(6), C(51)-Ga(1)-N(32) 106.86(7), C(55)-Ga(1)-N(32) 107.62(7).

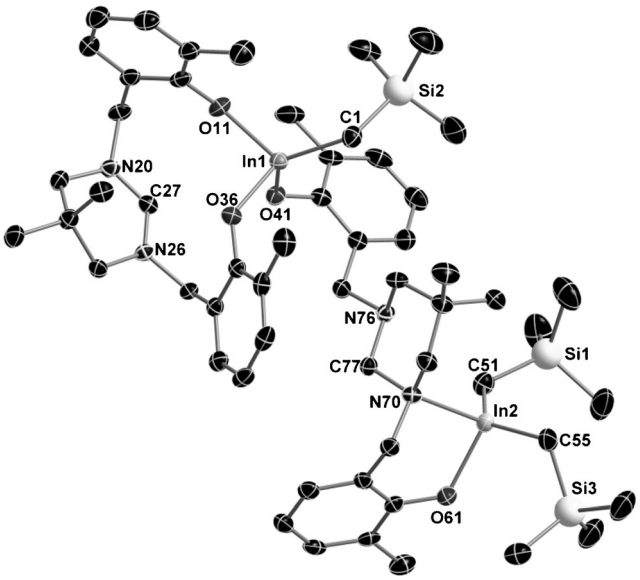

Figure 5. Molecular structure of the mixed zwitterionic/neutral-at-metal bimetallic indium complex **9** in the solid state, showing only the main component of the disordered SiMe$_3$ fragment. Hydrogen atoms and noninteracting solvent (toluene) are omitted for clarity. Ellipsoids are drawn at the 50% probability level. Pertinent bond lengths [Å] and angles [°]: In(1)–O(11) 2.050(2), In(1)–O(36) 2.058(2), In(1)–O(41) 2.087(2), In(1)–C(1) 2.142(3), In(2)–O(61) 2.095(2), In(2)–C(51) 2.153(4), In(2)–C(55) 2.155(4), In(2)–N(70) 2.357(3); C(27)-N(20)-C(21) 119.6(3), C(27)-N(20)-C(19) 121.4(3), C(21)-N(20)-C(19) 118.3(3), C(27)-N(26)-C(25) 121.9(3), C(27)-N(26)-C(28) 119.4(3), C(25)-N(26)-C(28) 118.6(3).

geometry in this inert complex. The coordination sphere around gallium comprises the two alkyl groups (C(51) and C(55)), the O$_{phenolate}$ atom (O(41)), and a single nitrogen atom from the hydropyrimidine cycle (N(32)). In particular, the potentially reactive phenol moiety does not bind to the metal atom, but is instead very remote, HO$_{phenol}$···Ga = 6.41 Å; such an arrangement does not favor further intramolecular reactivity, towards either a zwitterion or a neutral-at-metal complex, although intermolecular reactivity remains feasible with such complexes. For instance, the mixed bimetallic indium complex {^{Me}ON^(CH$^+$)^NO^{Me}}In$^-$(CH$_2$SiMe$_3$)–{^{Me}ON^(CH$_2$)NO^{Me}}–In-(CH$_2$SiMe$_3$)$_2$ (**9**) having zwitterionic and neutral-at-metal In atoms was isolated in small quantity during the synthesis of **6**. The arrangement of the salan ligand linking the two indium atoms in the byproduct **9** (Figure 5) is very similar to that of the ligand in **7-H** whereas the geometrical features of the zwitterionic part match those in **3**; its formation is attributed to the deleterious reaction of **6** with **8-H**,[26] the structure of which must be similar to that of **7-H** (Scheme 5). Attempts to isolate substantial amounts of the putative **8-H** and of **9** were unsuccessful.

Based on all the above experimental observations, we concluded that: 1) elimination of SiMe$_4$ by protonolysis occurs before the abstraction of hydride; 2) the presence of a second phenolic moiety in the direct vicinity of the metal center is required to remove the hydride from the hydropyrimidine core in an intramolecular process; 3) the passage from complexes such as **8-H** to the corresponding zwitterions (**6** in this case) does not involve a stable, long-lived metal-hydride transient species, from which H$_2$ would be delivered by recombination with the remaining phenolic proton; 4) in order to generate coordinatively saturated tetrahedral In (or Ga) complexes such as **7-H** and the like, bind-

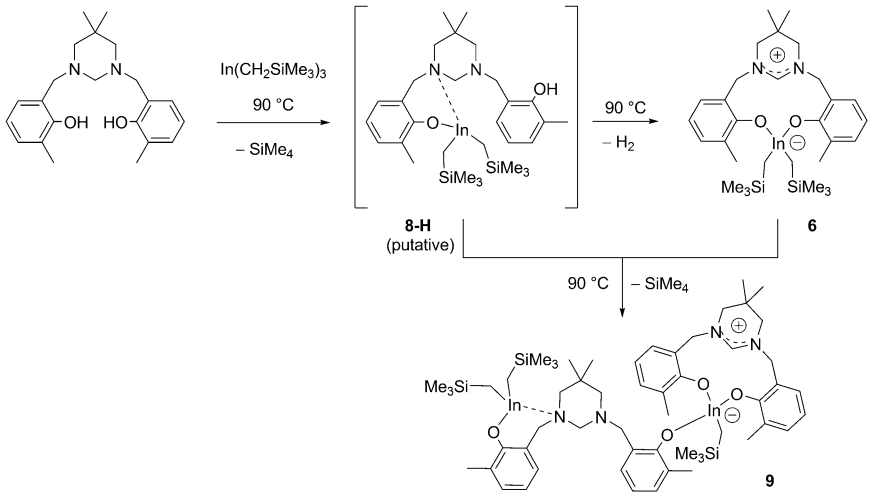

Scheme 5. Proposed pathway for the formation of the mixed zwitterionic/neutral-at-metal bimetallic indium complex **9**.

ing of the phenol OH moiety is less favorable than that of a $N_{hydropyrimidine}$ atom; and 5) the ability to form zwitterions varies with metal size and polarizing ability: the observed reactivity trend contrasts with these three metals' matching ability to promote halide abstraction in phosphine–trielane gold(I) complexes.[15,27]

Computational studies

Theoretical computations performed on the {ON^(CH_2)^NO}H_2/MR_3 systems corroborate these experimental observations.[16] In the case of aluminum (Figure 6), starting from the entry point $\mathbf{E_0}$ (viz. the proteo-ligand + Al_2Me_6), the first protonolysis leading to $\mathbf{AlR_1T_1f}$ takes place relatively easily and proceeds via a transition state $\mathbf{AlR_1T_1}$ (the monophenol–$AlMe_3$ adduct) of relatively low free energy, approximately 17.4 kcal mol^{-1}; note that the aluminate intermediate $\mathbf{AlR_1T_1f}$ with a protonated ammonium is kinetically more available than its neutral monophenolate derivative (i.e., the aluminum analogue of **7-H**). From $\mathbf{AlR_1T_1f}$, further reactivity can potentially follow two pathways. Computations predict that the route leading to the formation of the neutral-at-metal $\mathbf{AlR_4T_2f}$ (a product of general formula {ON^(CH_2)^NO}AlMe, i.e., the monometallic version of $\mathbf{[1]_2}$; Figure 6, plain line) is favored over that leading to the zwitterionic $\mathbf{AlR_1T_3f}$ (viz. the Al analogue of **2** and **3**; dashed line) both on kinetic and thermodynamic grounds. The transition state $\mathbf{AlR_4T_2}$ leading to the neutral-at-metal $\mathbf{AlR_4T_2f}$ is of lower energy ($\Delta G^{\neq} = -11.6$ kcal mol^{-1}) than that leading to $\mathbf{AlR_1T_2f}$ (a putative Al-hydride intermediate; transition state $\mathbf{AlR_1T_2}$, $\Delta G^{\neq} = -7.2$ kcal mol^{-1}) and ultimately $\mathbf{AlR_1T_3f}$ (transition state $\mathbf{AlR_1T_3}$, $\Delta G^{\neq} = -0.9$ kcal mol^{-1}); moreover, the computed product $\mathbf{AlR_4T_2f}$ is also much more stable than $\mathbf{AlR_1T_3f}$, with a difference of 18.0 kcal mol^{-1} in favor of the former. Note that only the monometallic $\mathbf{AlR_4T_2}$ was modeled for the economy of computing time, and the experimentally observed bimetallic $\mathbf{[1]_2}$ is likely to be substantially more stable, even if the energy of the associated transition state is expected to be of the same magnitude as that determined for $\mathbf{AlR_4T_2}$. DFT calculations thus indicate that the formation of a zwitterionic aluminum complex is unfavorable, which agrees with the experimental observations. Note that the transition state $\mathbf{AlR_4T_2}$ leading to the formation of the neutral-at-metal product by protonolysis of an Al–CH_3 bond is predicted to consist of a five-coordinated aluminum atom, with coordination of the phenolic OH moiety onto the metal.

The scenario is different for gallium (Figure 7). In this case the formation of the four-coordinated neutral-at-metal complex $\mathbf{GaR_4T_2f}$ (a putative monometallic complex of formula {ON^(CH_2)^NO}$GaCH_2SiMe_3$) is again thermodynamically slightly favored over the formation of the zwitterionic $\mathbf{GaR_1T_3f}$ (that is, **2** in its optimized geometry). However, the activation barrier leading to the formation of the thermodynamically more stable complex from the four-coordinated intermediate $\mathbf{GaR_1T_1f}$ (Figure 7, plain line) is now much greater ($\Delta G^{\neq} =$ 30.8 kcal mol^{-1}) than that affording the zwitterionic hydride $\mathbf{GaR_1T_2f}$ ($\Delta G^{\neq} = 18.9$ kcal mol^{-1}, dashed line). From $\mathbf{GaR_1T_2f}$, formation of the final zwitterion $\mathbf{GaR_1T_3f}$ occurs readily ($\Delta G^{\neq} =$ 12.9 kcal mol^{-1}).

On the basis of these computations, one can therefore assume that the formation of zwitterion **2** observed experimentally occurs owing to a largely favorable kinetic control. Note that: 1) starting from $\mathbf{GaR_1T_1f}$, attempts to converge towards a stable four- or five-coordinated neutral Ga···OH_{phenol} adduct (a requisite for the production of a neutral-at-metal Ga complex akin to $\mathbf{GaR_4T_2f}$) failed, as the system systematically relaxed back to more stable four-coordinated Ga···N species free of interactions with the phenolic OH moiety; and 2) the geometry around the tetrahedral metal in the intermediate $\mathbf{GaR_1T_1f}$ is similar to that observed experimentally by X-ray diffraction crystallography in the related **7-H**.

Computations suggest that kinetic control also governs the formation of the indium zwitterion **3** (Figure 8). Whereas the neutral-at-metal $\mathbf{InR_4T_2f}$ is estimated to be nominally more stable than the zwitterion

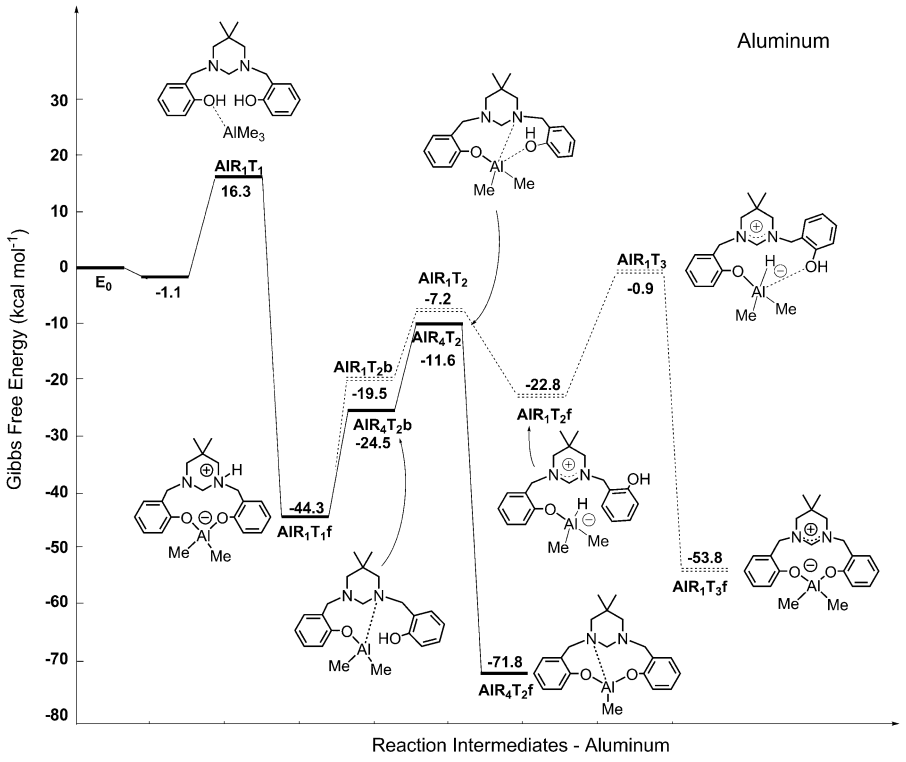

Figure 6. Computed pathways for the formation of aluminum zwitterionic (dashed line) versus neutral-at-metal model monometallic complex (plain line); $\mathbf{E_0} = {}^1/_2Al_2Me_6 + \{ON^(CH_2)^NO\}H_2$.

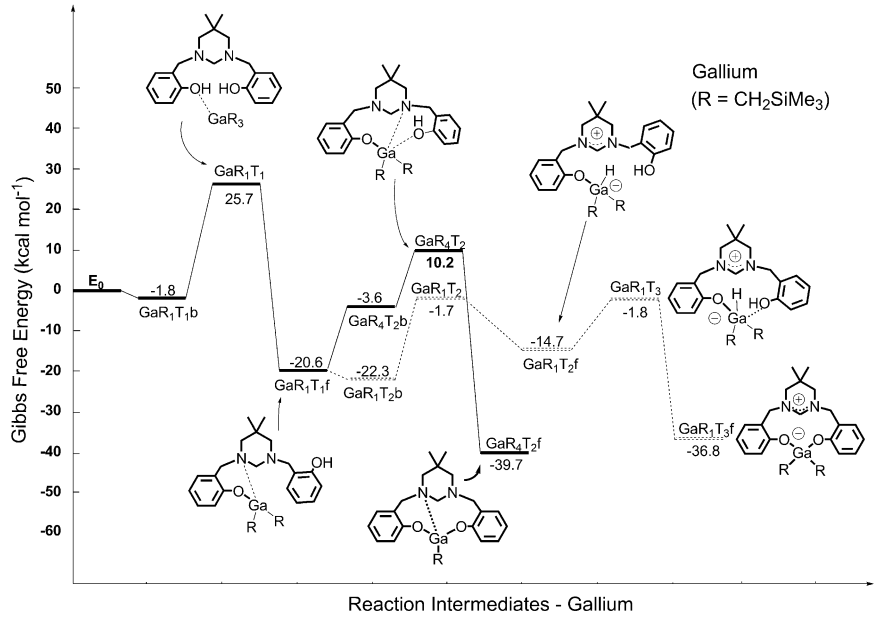

Figure 7. Computed pathways for the formation of gallium zwitterionic (dashed line) versus neutral-at-metal model monometallic complex (plain line); $\mathbf{E_0} = Ga(CH_2SiMe_3)_3 + \{ON\text{^}(CH_2)\text{^}NO\}H_2$.

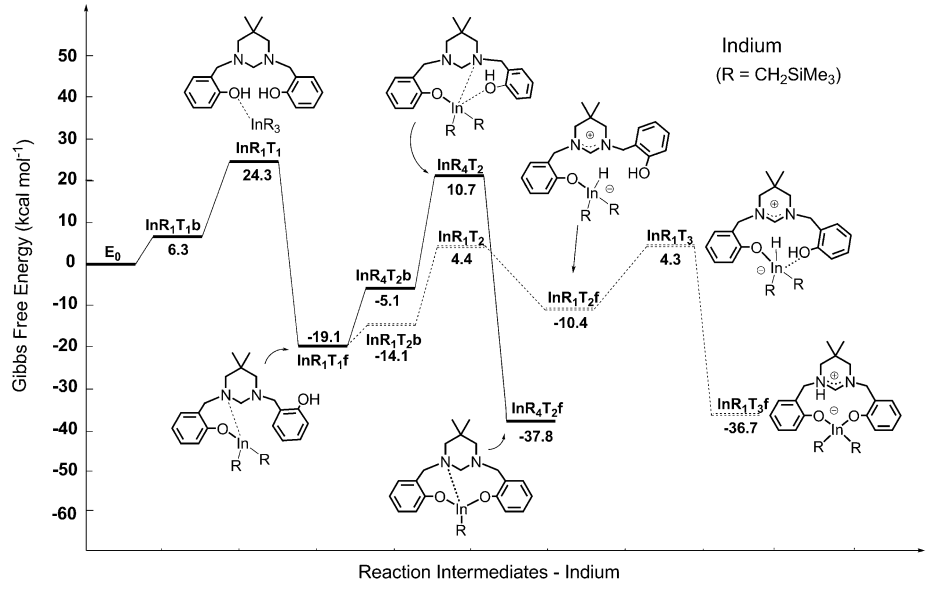

Figure 8. Computed pathways for the formation of indium zwitterionic (dashed line) versus neutral-at-metal model monometallic complex (plain line); $\mathbf{E_0} = In(CH_2SiMe_3)_3 + \{ON\text{^}(CH_2)\text{^}NO\}H_2$.

InR_1T_3f (that is, the geometrically optimized version of **3**) within the limits of the calculation method, from the tetrahedral N-coordinated intermediate **InR_1T_1f** the activation energy required to yield the former is again substantially higher (Figure 8, plain line; $\Delta G^{\neq} = 29.8$ kcal mol^{-1}) than that for the generation of the zwitterionic [In]-H transient species **InR_1T_2f** ($\Delta G^{\neq} = 23.5$ kcal mol^{-1}) and, from there, to the final zwitterion **InR_1T_3f** following release of dihydrogen ($\Delta G^{\neq} = 14.7$ kcal mol^{-1}, dashed line). As for Ga, starting from **InR_1T_1f** (which is accessed from the entry point via a transition state relatively high in free energy, $\Delta G^{\neq} = 24.3$ kcal mol^{-1}), we have been unable to identify resilient In···HO_{phenol} adducts.

Figure S26 (see the Supporting Information) summarizes the outcome of DFT computations, highlighting the different paths leading to neutral-at-metal aluminum and zwitterionic gallium and indium complexes. These results are fully compatible with the experimental data. All proceed through a first four-coordinated monophenolate neutral complex, in which coordination of a $N_{hydropyrimidine}$ atom is favorable over that of the $HO_{phenolic}$ moiety. Note that in the optimized metal-hydride intermediates **GaR_1T_2f** and **InR_1T_2f**, the phenolic proton is ideally oriented towards the M–H hydritic moiety, which facilitates the elimination of H_2. The calculations suggest that these intermediates are less stable than their neutral-at-metal monophenolate parents **GaR_1T_1f** and **InR_1T_1f**, respectively; this is consistent with the fact that the formation of an In-hydride species could not be detected upon heating **8-Me**, for which the formation of a zwitterion is precluded owing to the absence of a second phenolic proton.

The DFT computations are also in agreement with the experiments in the case of Ga-$(CH_2SiMe_3)_3$ and the bulkier *ortho*-Me-substituted proteoligand $\{^{Me}ON\text{^}(CH_2)\text{^}NO^{Me}\}H_2$. The robust **7-H** (the analogue to **GaR_1T_1f** in Figures 7 and S26 in the Supporting Information) formed with $Ga(CH_2SiMe_3)_3$ does not evolve further towards either the expected zwitterion or a neutral-at-metal complex (see Scheme 4). The computed activation barriers for both reactions ($\Delta G^{\neq} = 30.0$ and 40.9 kcal mol^{-1}, respectively) are much greater than those for the corresponding events calculated above for the less bulky $\{ON\text{^}(CH_2)\text{^}NO\}H_2$, and kinetic control thus prevents further evolution of the system in either direction. Regarding the system In-$(CH_2SiMe_3)_3/\{^{Me}ON\text{^}(CH_2)\text{^}NO^{Me}\}H_2$, from the first neutral-at-metal monophenolate intermediate both the formation of the neutral-at-metal ($\Delta G = -34.0$ kcal mol^{-1}) and zwitterion **6**

($\Delta G = -15.5$ kcal mol^{-1}) are thermodynamically feasible, but the production of the zwitterion is actually favored because of a lower activation energy ($\Delta G^{\neq} = 21.0$ and 18.0 kcal mol^{-1}, respectively).

Conclusion

Indium and, to a lesser extent, gallium hydrocarbyls afford original zwitterionic complexes upon treatment with salan proteo-ligands rigidified by a cyclic hydropyrimidine core through an unusual process of intramolecular hydride abstraction from α-amino C_{sp^3}–H moieties. These Ga and In zwitterions are obtained by release of H_2, which was detected experimentally. Since they are structurally and configurationally very rigid, it is tempting to consider the whole process as the reverse of H_2 activation by frustrated Lewis pairs (FLPs),[28] and it is particularly related to the metal FLPs described by Wass and co-workers[29] and Uhl and co-workers.[30] Major differences in the reactivity are observed on moving from aluminum, which simply affords the (expected) neutral-at-metal complexes by double protonolysis, to gallium and indium, for which the ease of hydride abstraction, release of dihydrogen, and formation of zwitterionic species varies with the metal size and corresponding polarizing ability. It is intriguing that the ability to carry out this hydride abstraction is apparently inversely proportional to the M–H bond enthalpies for Al (67 kcal mol^{-1}), Ga (62 kcal mol^{-1}), and In (54 kcal mol^{-1}).[31] These findings contrast with previous reports in which the three metals displayed comparable ability in promoting activation reactions.[12,16,17] DFT computations suggest that the outcome of the reactions is governed by a strict kinetic control, and a plausible reaction pathway based on experimental and DFT results is illustrated in Scheme 6 for the system $M(CH_2SiMe_3)_3$/{ON^(CH$_2$)^NO}H$_2$ (M = Ga, In), which generates the zwitterionic complexes **2** and **3**.

Despite repeated attempts and the bespoke synthesis of the monophenol {Me^^{Me}ON^(CH$_2$)^NO^{Me}}H, we have not been able to isolate metal-hydride intermediates or models; this is in line with the high reactivity of such hydrometalate species suggested by the DFT computations. Yet, this unusual C–H activation process and eventual formation of a carbocationic moiety opens the route towards nucleophilic functionalization of the pentahydropyrimidinium core.[32]

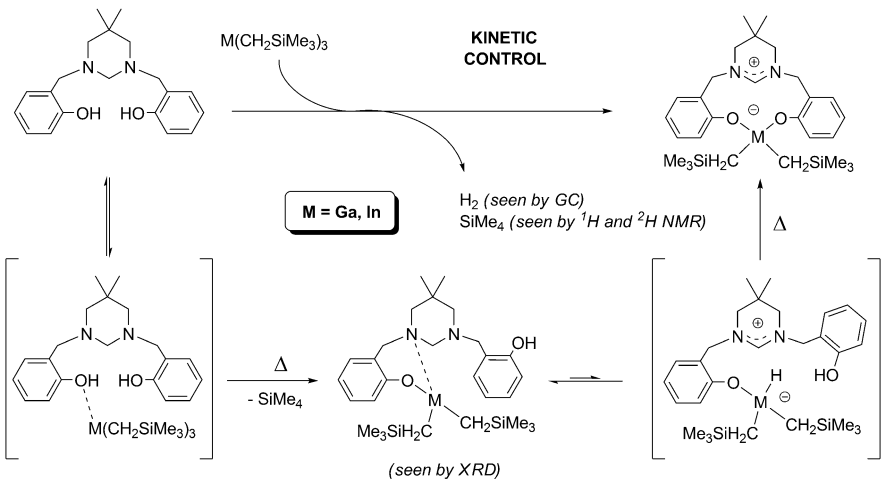

Scheme 6. Plausible reaction pathway for the formation of zwitterionic gallium/indium complexes.

Experimental Section

All manipulations were performed under inert atmosphere using standard Schlenk techniques or in a dry, solvent-free glovebox (Jacomex; $O_2 < 1$ ppm, $H_2O < 5$ ppm). $AlMe_3$ (2.0 M in toluene, Aldrich) was used as purchased. THF was distilled under argon from Na/benzophenone prior to use. Other solvents (pentane, toluene, dichloromethane, Et_2O) were collected from MBraun SPS-800 purification alumina columns. Deuterated solvents (Eurisotop, Saclay, France) were stored in sealed ampoules over activated 3 Å molecular sieves and degassed by several freeze–thaw cycles. $Ga(CH_2SiMe_3)_3$ and $In(CH_2SiMe_3)_3$ were prepared following literature procedures.[33]

NMR spectra were recorded on Bruker AM-400 and AM-500 spectrometers. All chemical shifts (given in ppm) were determined using residual signals of the deuterated solvents and were calibrated versus $SiMe_4$. Assignment of the signals was carried out using 1D (^{1}H, ^{13}C{^{1}H}) and 2D (COSY, HMBC, HMQC) NMR experiments.

Elemental analyses were performed on a Carlo Erba 1108 Elemental Analyser instrument at the London Metropolitan University by Stephen Boyer and were the average of a minimum of two independent measurements.

FTIR spectra were recorded between 400 and 4000 cm^{-1} as a powder on a Shimadzu IRAffinity-1 spectrometer equipped with an attenuated total reflectance module.

Crystals of {ON^(CH$_2$)^NO}H$_2$, **[1]$_2$**, **2**, **3·Et$_2$O**, and **7-H** suitable for X-ray diffraction analysis were obtained by recrystallization of the purified compound; crystals of **9** were isolated as byproducts during the synthesis of **6**. Diffraction data were collected at 150(2) K by using a Bruker APEX CCD diffractometer with graphite-monochromated $Mo_{K\alpha}$ radiation ($\lambda = 0.71073$ Å). A combination of ω and Φ scans was carried out to obtain at least a unique data set. The crystal structures were solved by direct methods, and remaining atoms were located from difference Fourier synthesis followed by full-matrix least-squares refinement based on F2 (programs SIR97 and SHELXL-97).[34] Carbon- and oxygen-bound hydrogen atoms were placed at calculated positions and forced to ride on the attached atom. All non-hydrogen atoms were refined with anisotropic displacement parameters. The locations of the largest peaks in the final difference Fourier map calculation as well as the magnitude of the residual electron densities were of no chemical significance. Relevant collection and refinement data are given in the Supporting Information. CCDC-980041 ({ON^(CH$_2$)^NO}H$_2$), 980042 (**[1]$_2$**), 980043 (**2**), 980044 (**3·Et$_2$O**), 980045 (**7-H**), 987689 ({$_{tBu}$ON^(CH$_2$)^NO$_{tBu}$}H$_2$), 987690 (**5**), 987691 ({ON^(CHPh)^NO}H$_2$), 987692 ({$_{Me}$ON^(CHPh)^NO$_{Me}$}H$_2$), 987693 ({$_{Me}$ON^(CH$_2$)^NO$_{Me}$}H$_2$), 987694 ({{{$_{Me}$ON^(CH$_2$)^NO$_{Me}$}Li–Li{THF}$_2$}$_2$}), and 987695 (**9**·toluene) contain the supplementary crystallographic data for this paper.

These data can be obtained free of charge from The Cambridge Crystallographic Data Centre via www.ccdc.cam.ac.uk/data_request/cif.

{ONNO}H_2

2,2-Dimethylpropane-1,3-diamine (5.1 g, 50 mmol) was dissolved in ethanol (120 mL) and salicylaldehyde (10.7 mL, 100 mmol) was added slowly. The reaction mixture was heated at reflux for 1 h. After cooling to 0 °C, $NaBH_4$ was added (7.6 g, 200 mmol; 4 equiv) in portions and the reaction mixture was stirred at room temperature for 1 h. Water (200 mL) was added and the mixture was stirred for another hour. The product was extracted with CH_2Cl_2, the organic phase was dried over $MgSO_4$, and the volatiles were pumped off to give {ONNO}H_2 as a colorless solid. Yield: 15.2 g, 97%. {^{Me}ONNO^{Me}}H_2 and {^{tBu}ONNO^{tBu}}H_2 were synthesized by following the same procedure with the appropriate substituted salicylaldehyde.

{ON^(CH_2)^NO}H_2

{ONNO}H_2 (6.00 g, 19.1 mmol) was dissolved in acetonitrile (ca. 150 mL), and formaldehyde (14.3 mL of a 37% aqueous solution, 191 mmol, 10 equiv) was added by syringe. The reaction mixture was stirred for 24 h at room temperature, which resulted in the precipitation of a colorless solid. The solid was isolated by filtration and washed with cold acetonitrile (3×15 mL) and pentane (2×5 mL). {ON^(CH_2)^NO}H_2 was obtained as a colorless powder upon drying to constant weight. Yield: 4.68 g, 75%. ^{1}H NMR (C_6D_6, 343 K, 500.13 MHz): δ = 9.94 (s, 2H; C_{arom}-O*H*), 7.09 (t, $^3J_{HH}$ = 7.7 Hz, 2H; C_{arom}*H*), 7.04 (d, $^3J_{HH}$ = 7.3 Hz, 2H; C_{arom}*H*), 6.78 (d, $^3J_{HH}$ = 7.9 Hz, 2H; C_{arom}*H*), 6.71 (t, $^3J_{HH}$ = 7.3 Hz, 2H; C_{arom}*H*), 3.17 (s, 4H; NCH_2-C_{arom}), 2.72 (br s, 2H; NCH_2N), 1.83 (s, 4H; CH_2C(CH_3)$_2$CH_2), 0.71 ppm (s, 6H; CH_3); ^{13}C{^{1}H} NMR (C_6D_6, 343 K, 125.75 MHz): δ = 158.3 (C_{arom}-OH), 129.1 (C_{arom}H), 128.4 (C_{arom}H), 120.6 (C_{arom}-CH_2N), 118.9 (C_{arom}H), 116.6 (C_{arom}H), 74.5 (NCH_2N), 63.4 (CH_2C(CH_3)$_2$CH_2), 58.5 (NCH_2-C_{arom}), 30.4 ($CH_2C(CH_3)_2CH_2$), 25.1 ppm ($CH_2C(CH_3)_2CH_2$); ESI-HRMS: *m/z* calcd for $[M+H]^+$: 327.20725; found: 327.2070 (1 ppm); elemental analysis calcd (%) for $C_{20}H_{26}N_2O_2$ (326.46 g mol^{-1}): C 73.6, H 8.0, N 8.6; found: C 73.4, H 7.7, N 8.4. The other proteo-ligands were obtained by following a similar procedure using various aldehydes and *ortho*-substituted phenols.[16]

[{ON^(CH_2)^NO}AlMe_2]$_2$ ([1]$_2$)

{ON^(CH_2)^NO}H_2 (300 mg, 0.92 mmol) was dissolved in toluene (15 mL) by heating the solution at 60 °C. Then, this solution was added dropwise to $AlMe_3$ (0.54 mL of a 2.0 M toluene solution, 0.92 mmol) diluted in toluene (2 mL). The reaction mixture was stirred at 70 °C for 7 h. The volatiles were then pumped off to give a colorless solid, which was washed with pentane (3×7 mL). The resulting colorless powder was dried under high vacuum. Finally, the expected product was crystallized from hot benzene by slow decrease of the temperature, from 90 °C to room temperature. Yield: 650 mg, 97%. This reaction was also carried out in THF with the same outcome. ^{1}H NMR (C_6D_6, 343 K, 500.13 MHz): δ = 7.14 (dd, $^3J_{HH}$ = 8.5, $^4J_{HH}$ = 0.9 Hz, 4H; C_{arom}*H*), 7.07 (d, $^3J_{HH}$ = 8.5 Hz, 4H; C_{arom}*H*), 6.74 (dd, $^3J_{HH}$ = 7.2, $^4J_{HH}$ = 0.9 Hz, 4H; C_{arom}*H*), 6.66 (td, $^3J_{HH}$ = 7.2, $^4J_{HH}$ = 0.9 Hz, 4H; C_{arom}*H*), 3.96 and 2.62 (AX system, $^2J_{HH}$ = 11.6 Hz, 4H; NCH_2N), 3.62 and 3.02 (AB system, $^2J_{HH}$ = 13.5 Hz, 8H; NCH_2-C_{arom}), 2.46 and 1.83 (AX system, $^2J_{HH}$ = 12.8 Hz, 8H; CH_2C(CH_3)$_2$CH_2), 0.73 (s, 6H; $CH_2CCH_3(CH_3)CH_2$), 0.39 (s, 6H; $CH_2CCH_3(CH_3)CH_2$), −0.33 ppm (s, 6H; Al-CH_3); ^{13}C{^{1}H} NMR (C_6D_6, 343 K, 125.75 MHz): δ = 160.2 (C_{arom}-OAl), 130.6 (C_{arom}H), 129.4 (C_{arom}H), 124.6 (C_{arom}-CH_2N), 120.7 (C_{arom}H), 118.3 (C_{arom}H), 74.2 (NCH_2N), 63.9 (NCH_2-C_{arom}), 58.9 (CH_2C(CH_3)$_2$CH_2), 31.4 ($CH_2C(CH_3)_2CH_2$), 27.3 ($CH_2CCH_3(CH3)CH_2$), 26.2 ppm ($CH_2CCH_3(CH3)CH_2$), no visible Al-CH_3; elemental analysis calcd (%) for $C_{42}H_{54}Al_2N_4O_4$ (732.85 g mol^{-1}): C 68.8, H 7.4, N 7.6; found: C 68.9, H 7.1, N 7.9.

{ON^(CH^+)^NO}Ga$^-$(CH_2SiMe_3)$_2$ (2)

{ON^(CH_2)^NO}H_2 (140 mg, 0.43 mmol) and Ga(CH_2SiMe_3)$_3$ (142 mg, 0.43 mmol) were dissolved in THF (10 mL). The reaction mixture was stirred at 100 °C for 90 h. Then, the volatiles were pumped off, the product was extracted with diethyl ether (2×5 mL), the solvent was removed, and the solid was washed with pentane (3×3 mL) and dried under high dynamic vacuum affording **2** as a colorless solid. Yield: 112 mg, 46%. ^{1}H NMR (C_6D_6, 315 K, 500.13 MHz): δ = 7.92 (s, 1H; NC*H*N), 7.31 (td, $^3J_{HH}$ = 8.3, $^4J_{HH}$ = 1.9 Hz, 2H; C_{arom}*H*), 7.03 (dd, $^3J_{HH}$ = 8.3, $^4J_{HH}$ = 1.1 Hz, 2H; C_{arom}*H*), 6.82 (dd, $^3J_{HH}$ = 7.3, $^4J_{HH}$ = 1.9 Hz, 2H; C_{arom}*H*), 6.66 (td, $^3J_{HH}$ = 7.3, $^4J_{HH}$ = 1.1 Hz, 2H; C_{arom}*H*), 3.76 (s, 4H; NCH_2-C_{arom}), 1.93 (s, 4H; CH_2C(CH_3)$_2$CH_2), 0.45 (s, 18H; Si(CH_3)$_3$), 0.03 (s, 6H; $CH_2C(CH_3)_2CH_2$), −0.08 ppm (s, 4H; GaCH_2Si); ^{13}C{^{1}H} NMR (C_6D_6, 298 K, 125.75 MHz): δ = 165.3 (C_{arom}-OGa), 153.7 (NCHN), 130.9 (C_{arom}H), 130.2 (C_{arom}H), 120.4 (C_{arom}H), 120.2 (C_{arom}-CH_2N), 114.1 (C_{arom}H), 57.8 (NCH_2-C_{arom}), 51.9 (CH_2-C(CH_3)$_2$CH_2), 26.0 ($CH_2C(CH_3)_2CH_2$), 22.8 ($CH_2C(CH_3)_2CH_2$), 2.5 (Si(CH_3)$_3$), −0.4 ppm (InCH_2Si); ^{15}N NMR (C_6D_6, 298 K, 40.5 MHz): 113.4 ppm (*N*CH_2-C_{arom}); elemental analysis calcd (%) for $C_{28}H_{45}GaN_2O_2Si_2$ (567.56 g mol^{-1}): C 59.3, H 8.0, N 4.9; found: C 59.0, H 8.0, N 5.1.

{ON^(CH^+)^NO}In$^-$(CH_2SiMe_3)$_2$ (3)

{ON^(CH_2)^NO}H_2 (200 mg, 0.61 mmol) and In(CH_2SiMe_3)$_3$ (230 mg, 0.61 mmol) were dissolved in THF (10 mL). The reaction mixture was stirred at 70 °C for 22 h. The volatiles were then pumped off to afford a solid, which was dried under vacuum. The title product was extracted using diethyl ether (3×3 mL), washed with pentane (2×3 mL), and dried under high vacuum. Yield: 288 mg, 77%. ^{1}H NMR (C_6D_6, 315 K, 400.16 MHz): δ = 7.96 (s, 1H; NC*H*N), 7.27–7.25 (m, 2H; C_{arom}*H*), 6.88 (dd, $^3J_{HH}$ = 8.2, $^4J_{HH}$ = 1.0 Hz, 2H; C_{arom}*H*), 6.82 (dd, $^3J_{HH}$ = 7.26, $^4J_{HH}$ = 1.82 Hz, 2H; C_{arom}*H*), 6.60 (td, $^3J_{HH}$ = 7.28, $^4J_{HH}$ = 1.11 Hz, 2H; C_{arom}*H*), 3.82 (s, 4H; NCH_2-C_{arom}), 1.99 (s, 4H; CH_2C(CH_3)$_2$CH_2), 0.39 (s, 18H; Si(CH_3)$_3$), 0.07 (s, 6H; $CH_2C(CH_3)_2CH_2$), 0.01 ppm (s, 4H; InCH_2Si); ^{13}C{^{1}H} NMR (C_6D_6, 315 K, 100.62 MHz): δ = 167.2 (C_{arom}-OIn), 153.0 (NCHN), 131.0 (C_{arom}H), 130.4 (C_{arom}H), 120.3 (C_{arom}-CH_2N), 120.2 (C_{arom}H), 113.2 (C_{arom}H), 57.5 (NCH_2-C_{arom}), 52.0 ($CH_2C(CH_3)_2CH_2$), 25.9 ($CH_2C(CH_3)_2CH_2$), 22.7 ($CH_2C(CH_3)_2CH_2$), 2.5 (Si(CH_3)$_3$), 0.1 ppm (InCH_2Si); elemental analysis calcd (%) for $C_{28}H_{45}InN_2O_2Si_2$ (612.66 g mol^{-1}): C 54.9, H 7.4, N 4.7; found: C 54.0, H 7.6, N 4.9. Satisfactory elemental analysis was not obtained for C, most likely because of the presence of a substantial amount of Si leading to the formation of SiC.

[{^{Me}ON^(CH_2)^NO^{Me}}AlMe_2]$_2$ ([4]$_2$)

{^{Me}ON^(CH_2)^NO^{Me}}H_2 (100 mg, 0.28 mmol) was dissolved in toluene (4 mL), a 2.0 M $AlMe_3$ solution in toluene (140 μL, 0.28 mmol) was diluted in toluene (1 mL), and then the solution of proligand was added dropwise onto the solution of $AlMe_3$ at room temperature resulting in the release of methane. The reaction mixture was stirred at 70 °C for 7 h. After cooling the reaction medium to room temperature, the volatiles were pumped off. The resulting solid was washed with pentane (2×1 mL) and dried under dynamic vacuum for several hours. ^{1}H NMR (C_6D_6, 298 K, 500.13 MHz): δ = 7.15–7.13 (m, 4H; C_{arom}*H*), 6.74–6.68 (m, 8H; C_{arom}*H*), 4.01 and 2.57 (AX system, $^2J_{HH}$ = 11.5 Hz, 4H; NCH_2N), 3.55 and 2.98 (AX system,

$^2J_{HH}$ = 13.7 Hz, 8H; NCH_2-C$_{arom}$), 2.50 (s, 12H; C$_{arom}$-CH_3), 2.35 and 1.70 (AX system, $^2J_{HH}$ = 12.9 Hz, 8H; CH_2C(CH$_3$)$_2$CH_2), 0.68 (s, 6H; CH$_2$CCH_3(CH$_3$)CH$_2$), 0.31 (s, 6H; CH$_2$CCH$_3$(CH_3)CH2), −0.25 ppm (s, 6H; Al-CH_3); ^{13}C{^{1}H} NMR (C$_6$D$_6$, 298 K, 125.75 MHz): δ = 158.3 (C$_{arom}$-OAl), 131.6 (C$_{arom}$H), 128.3 (C$_{arom}$-CH$_3$), 127.4 (C$_{arom}$H), 123.8 (C$_{arom}$CH$_2$N), 118.0 (C$_{arom}$H), 74.0 (NCH$_2$N), 63.4 (CH$_2$C(CH$_3$)$_2$CH$_2$), 58.9 (NCH$_2$-C$_{arom}$), 31.2 (CH$_2$C(CH$_3$)$_2$CH$_2$), 27.1 (CH$_2$CCH$_3$(CH$_3$)CH$_2$), 25.9 (CH$_2$CCH$_3$(CH$_3$)CH$_2$), 17.1 (C$_{arom}$-C(CH$_3$), −11.6 ppm (br, Al-CH$_3$); elemental analysis calcd (%) for C$_{46}$H$_{62}$Al$_2$N$_4$O$_4$ (788.97 g mol^{-1}): C 70.0, H 7.9, N 7.1; found: C 69.9, H 7.8, N 7.0.

{ON^(CPh$^+$)^NO}In$^-$(CH$_2$SiMe$_3$)$_2$ (5)

{ON^(CHPh)^NO}H$_2$ (250 mg, 0.62 mmol) and In(CH$_2$SiMe$_3$)$_3$ (233 mg, 0.62 mmol) were dissolved in THF (8 mL) and stirred at 80 °C. After 3.5 days, the volatiles were removed under vacuum. The isolated solid was washed with pentane (3×3 mL) and dried under high vacuum, affording **5** as a colorless solid. Yield: 275 mg, 66%. ^{1}H NMR (C$_6$D$_6$, 298 K, 500.13 MHz): δ = 9.25 (dt, $^3J_{HH}$ = 7.9, $^4J_{HH}$ = 1.0 Hz, 1H; C$_{arom}$H), 7.48 (td, $^3J_{HH}$ = 7.5, $^4J_{HH}$ = 0.9 Hz, 1H; C$_{arom}$H), 7.28 (td, $^3J_{HH}$ = 7.7, $^4J_{HH}$ = 1.8 Hz, 2H; C$_{arom}$H), 7.11 (tt, $^3J_{HH}$ = 7.5, $^4J_{HH}$ = 1.2 Hz, 1H; C$_{arom}$H), 7.04 (td, $^3J_{HH}$ = 7.5, $^4J_{HH}$ = 0.9 Hz, 1H; C$_{arom}$H), 6.80 (dd, $^3J_{HH}$ = 7.9, $^4J_{HH}$ = 1.0 Hz, 2H; C$_{arom}$H), 6.70 (dd, $^3J_{HH}$ = 7.5, $^4J_{HH}$ = 1.8 Hz, 2H; C$_{arom}$H), 6.60 (m, 3H; C$_{arom}$H), 4.74 and 2.99 (AX system, $^2J_{HH}$ = 11.7 Hz, 4H; NCH_2-C$_{arom}$), 2.79 and 2.19 (AB system, $^2J_{HH}$ = 12.4 Hz, 4H; CH_2C(CH$_3$)$_2$CH_2), 0.51 (s, 9H; Si(CH_3)$_3$), 0.49 (s, 3H; CH$_2$CCH_3(CH$_3$)CH$_2$), 0.35 (s, 9H; Si(CH_3)$_3$), 0.24 (s, 2H; InCH_2Si), 0.16 (s, 3H; CH$_2$CCH$_3$(CH_3)CH$_2$), −0.40 ppm (s, 2H; InCH_2Si); ^{13}C{^{1}H} NMR (C$_6$D$_6$, 298 K, 125.75 MHz): δ = 166.9 (C$_{arom}$-OIn), 162.8 (*i*-C$_6$H$_5$), 133.6 (C$_{arom}$H), 131.0 (2×C$_{arom}$H), 130.8 (NC(Ph)N), 130.7 (C$_{arom}$H), 129.7 (C$_{arom}$H), 128.4 (C$_{arom}$H), 126.7 (C$_{arom}$H), 121.4 (C$_{arom}$-CH$_2$N), 120.4 (C$_{arom}$H), 114.1 (C$_{arom}$H), 58.5 (NCH$_2$-C$_{arom}$), 55.7 (CH$_2$C-(CH$_3$)$_2$CH$_2$), 26.8 (CH$_2$C(CH$_3$)$_2$CH$_2$), 24.5 (CH$_2$CCH$_3$(CH$_3$)CH$_2$), 22.8 (CH$_2$CCH$_3$(CH$_3$)CH$_2$), 2.8 (Si(CH$_3$)$_3$), 2.8 (Si(CH$_3$)$_3$), 2.3 (InCH$_2$Si), −1.2 ppm (InCH$_2$Si); elemental analysis calcd (%) for C$_{34}$H$_{49}$InN$_2$O$_2$Si$_2$ (668.75 g mol^{-1}): C 59.3, H 7.2, N 4.1; found: C 59.4, H 7.1, N 4.2.

{^{Me}ON^(CH$^+$)^NO^{Me}}In$^-$(CH$_2$SiMe$_3$)$_2$ (6)

{^{Me}ON^(CH$_2$)^NO^{Me}}H$_2$ (185 mg, 0.52 mmol) and In(CH$_2$SiMe$_3$) (196 mg, 0.52 mmol) were dissolved in THF (5 mL) and the reaction mixture heated at 90 °C for 90 h. After cooling to room temperature, the volatiles were pumped off, and the resulting solid was washed with pentane (2×3 mL) and dried under dynamic vacuum to afford a colorless powder. Despite several attempts at recrystallization, **6** could not be obtained with purity higher than 95%; a minor impurity, most likely corresponding to **9**, was always detected spectroscopically. ^{1}H NMR (C$_6$D$_6$, 298 K, 500.13 MHz): δ = 8.13 (s, 1H; NC*H*N), 7.28 (dd, $^3J_{HH}$ = 7.3, $^4J_{HH}$ = 1.8 Hz, 2H; C$_{arom}$H), 6.82 (dd, $^3J_{HH}$ = 7.3, $^4J_{HH}$ = 1.8 Hz, 2H; C$_{arom}$H), 6.67 (t, $^3J_{HH}$ = 7.3 Hz, 2H; C$_{arom}$H), 3.84 (s, 4H; NCH_2-C$_{arom}$), 2.50 (s, 6H; C$_{arom}$-CH_3), 1.94 (s, 4H; CH_2C(CH$_3$)$_2$CH_2), 0.32 (s, 18H; Si(CH_3)$_3$), 0.16 (s, 6H; CH$_2$C-(CH_3)$_2$CH$_2$), −0.05 ppm (s, 4H; InCH_2Si); ^{13}C{^{1}H} NMR (C$_6$D$_6$, 298 K, 125.75 MHz): δ = 166.2 (C$_{arom}$-OIn), 153.9 (NCHN), 132.9 (C$_{arom}$H), 129.2 (C$_{arom}$H), 128.4 (C$_{arom}$-CH$_3$), 120.7 (C$_{arom}$-CH$_2$N), 114.0 (C$_{arom}$H), 58.5 (NCH$_2$-C$_{arom}$), 53.3 (CH$_2$C(CH$_3$)$_2$CH$_2$), 26.7 (CH$_2$C(CH$_3$)$_2$CH$_2$), 23.4 (CH$_2$C(CH$_3$)$_2$CH$_2$), 19.6 (C$_{arom}$-CH$_3$), 2.9 (Si(CH$_3$)$_3$), 1.4 ppm (InCH$_2$Si). Satisfactory elemental analysis could not be obtained for this complex, most probably due to contamination by **9** and also the presence of a substantial amount of Si leading to the formation of SiC.

[{^{Me}ON^(CH$_2$)^NO^{Me}}H]Ga(CH$_2$SiMe$_3$)$_2$ (7-H)

{^{Me}ON^(CH$_2$)^NO^{Me}}H$_2$ (250 mg, 0.71 mmol) and Ga(CH$_2$SiMe$_3$)$_3$ (235 mg, 0.71 mmol) were dissolved in THF (9 mL) and heated at 70 °C for 50 h. The volatiles were next pumped off to afford a sticky solid. Stripping with pentane (3×2 mL) followed by drying in vacuo afforded **7-H** as a white solid. Yield: 400 mg, 95%. ^{1}H NMR (C$_6$D$_6$, 298 K, 500.13 MHz): δ = 9.49 (s, 1H; C$_{arom}$O*H*), 7.19 (d, $^3J_{HH}$ = 7.2 Hz, 1H; C$_{arom}$H), 7.05 (d, $^3J_{HH}$ = 7.5 Hz, 1H; C$_{arom}$H), 6.92 (d, $^3J_{HH}$ = 7.2 Hz, 1H; C$_{arom}$H), 6.74 (t, $^3J_{HH}$ = 7.5 Hz, 1H; C$_{arom}$H), 6.66 (m, 2H; C$_{arom}$H), 4.16 (s, 2H; NCH_2-C$_{arom}$), 3.55 and 2.73 (AX system, $^2J_{HH}$ = 11.1 Hz, 2H; NCH_2N), 3.10 and 2.73 (AX system, $^2J_{HH}$ = 13.4 Hz, 2H; CH_2C(CH$_3$)$_2$CH$_2$), 2.58 and 2.25 (AB system, $^2J_{HH}$ = 14.1 Hz, 2H; NCH_2-C$_{arom}$), 2.46 (s, 3H; C$_{arom}$-CH_3), 2.43 (s, 3H; C$_{arom}$-CH_3), 2.25 and 1.23 (AX system, $^2J_{HH}$ = 11.6 Hz, 2H; CH$_2$C(CH$_3$)$_2$CH_2), 0.92 (s, 3H; CH$_2$CCH_3(CH$_3$)CH$_2$), 0.33 (s, 9H; Si(CH_3)$_3$), 0.27 (s, 9H; Si(CH_3)$_3$), 0.21 (s, 3H; CH$_2$CCH$_3$(CH_3)CH$_2$), −0.40 (m, 2H; GaCH_2Si), −0.51 ppm (m, 2H; GaCH_2Si); ^{13}C{^{1}H} NMR (C$_6$D$_6$, 298 K, 125.75 MHz): δ = 161.4 (C$_{arom}$-OGa), 155.9 (C$_{arom}$-OH), 131.9 (C$_{arom}$H), 131.3 (C$_{arom}$H), 129.0 (C$_{arom}$H), 128.7 (C$_{arom}$-CH$_3$), 127.0 (C$_{arom}$H), 125.6 (C$_{arom}$-CH$_3$), 119.2 (C$_{arom}$H), 119.6 (C$_{arom}$-CH$_2$N), 118.4 (C$_{arom}$-CH$_2$N), 116.4 (C$_{arom}$H), 72.1 (NCH$_2$N), 63.6 (CH$_2$C(CH$_3$)$_2$CH$_2$), 58.8 (NCH$_2$-C$_{arom}$), 58.4 (CH$_2$C-(CH$_3$)$_2$CH$_2$), 57.4 (N′CH$_2$-C$_{arom}$), 30.5 (CH$_2$C(CH$_3$)$_2$CH$_2$), 28.2 (CH$_2$CCH$_3$-(CH$_3$)CH$_2$), 27.4 (CH$_2$CCH$_3$(CH$_3$)CH$_2$), 17.5 (C$_{arom}$-CH$_3$), 16.0 (C$_{arom}$-CH$_3$), 2.5 (Si(CH$_3$)$_3$), 2.4 (Si(CH$_3$)$_3$), −0.3 ppm (GaCH$_2$Si); elemental analysis calcd (%) for C$_{30}$H$_{51}$GaN$_2$O$_2$Si$_2$ (597.63 g mol^{-1}): C 60.3, H 8.6, N 4.7; found: C 59.9, H 8.7, N 4.6.

[{^{Me}ON^(CH$_2$)^NO^{Me}}D]Ga(CH$_2$SiMe$_3$)$_2$ (7-D)

Compound **7-D** was synthesized quantitatively in a J-Young NMR tube as described for **7-H** starting from [{^{Me}ON^(CH$_2$)^NO^{Me}}D$_2$ and Ga(CH$_2$SiMe$_3$)$_3$ in C$_6$D$_6$. All resonances matched those of **7-H** except for C$_{arom}$O*D*. ^{2}H NMR (C$_6$H$_6$, 298 K, 61.42 MHz): δ = 9.32 ppm (br, C$_{arom}$-O*D*).

{Me ^{Me}ON^(CH$_2$)^NO^{Me}}In(CH$_2$SiMe$_3$)$_2$ (8-Me)

{Me^^{Me}ON^(CH$_2$)^NO^{Me}}H$_2$ (200 mg, 0.54 mmol) and In(CH$_2$SiMe$_3$)$_3$ (203 mg, 0.54 mmol) were dissolved in THF (6 mL) and the reaction medium was stirred at 70 °C for 20 h. After cooling to room temperature, the volatiles were pumped off under vacuum. The resulting solid was purified by stripping with pentane (3×2 mL) and dried under dynamic vacuum to afford **8-Me** as a viscous oil. Yield: 315 mg, 96%. ^{1}H NMR (C$_6$D$_6$, 298 K, 500.13 MHz): δ = 7.34 (d, $^3J_{HH}$ = 7.3 Hz, 1H; C$_{arom}$H), 7.25 (d, $^3J_{HH}$ = 6.3 Hz, 1H; C$_{arom}$H), 6.97–6.89 (m, 3H; C$_{arom}$H), 6.74 (t, $^3J_{HH}$ = 7.3 Hz, 1H; C$_{arom}$H), 4.05 and 2.83 (AX system, one broad signal, $^2J_{HH}$ = 12.2 Hz, 2H; NCH_2-C$_{arom}$), 3.65 and 2.43 (AX system, one broad signal, $^2J_{HH}$ = 9.3 Hz, 2H; NCH_2N), 3.32 and 3.17 (AB system, $^2J_{HH}$ = 13.3 Hz, 2H; NCH_2-C$_{arom}$), 3.24 (s, 3H; C$_{arom}$-OCH_3), 2.59 and 1.51 (AX system, one broad signal, $^2J_{HH}$ = 12.6 Hz, 2H; CH_2C(CH$_3$)$_2$CH$_2$), 2.55 (s, 3H; C$_{arom}$-CH_3), 2.16 and 1.45 (br AX system, $^2J_{HH}$ = 11.3 Hz, 2H; CH$_2$C(CH$_3$)$_2$CH_2), 0.90 (s, 3H; CH$_2$CCH_3(CH$_3$)CH$_2$), 0.47 (s, 3H; CH$_2$CCH$_3$(CH_3)CH$_2$), 0.41 (s, 9H; Si(CH_3)$_3$), 0.31 (s, 9H; Si(CH_3)$_3$), 0.08–0.00 (AB system, $^2J_{HH}$ = 12.6 Hz, 2H; InCH_2Si), −0.12 to −0.23 ppm (AB system, $^2J_{HH}$ = 12.5 Hz, 2H; InCH_2Si); ^{13}C{^{1}H} NMR (C$_6$D$_6$, 298 K, 125.75 MHz): δ = 165.1 (C$_{arom}$-OIn), 157.8 (C$_{arom}$-OH), 132.1 (C$_{arom}$H), 131.3 (C$_{arom}$-CH$_3$), 130.9 (C$_{arom}$H), 129.8 (C$_{arom}$-CH$_2$N), 129.5 (C$_{arom}$H), 129.1 (C$_{arom}$-CH$_3$), 128.4 (C$_{arom}$H), 124.2 (C$_{arom}$H), 119.8 (C$_{arom}$-CH$_2$N), 114.7 (C$_{arom}$H), 77.1 (NCH$_2$N), 66.0 (CH$_2$C(CH$_3$)$_2$CH$_2$), 62.8 (CH$_2$C(CH$_3$)$_2$CH$_2$), 61.6 (NCH$_2$-C$_{arom}$), 60.2 (C$_{arom}$-OCH$_3$), 53.0 (NCH$_2$-C$_{arom}$), 31.5 (CH$_2$C(CH$_3$)$_2$CH$_2$), 27.0 (CH$_2$CCH$_3$(CH$_3$)CH$_2$), 26.9 (CH$_2$CCH$_3$(CH$_3$)CH$_2$), 17.5 (C$_{arom}$-CH$_3$), 16.2 (C$_{arom}$-CH$_3$), 2.9 (InCH$_2$), 2.7 (Si(CH$_3$)$_3$), 2.6 (Si(CH$_3$)$_3$), 2.1 ppm

($InCH_2Si$). No satisfactory elemental analysis was obtained for **8-Me**, most likely because of the presence of a substantial amount of Si leading to the formation of SiC.

DFT computations

All calculations were carried out at the DFT level using the B3PW91 functional in the Gaussian 09 code.[35] The equilibrium and transition structures were fully optimized at the Becke's three-parameter hybrid functional[36] combined with the nonlocal correlation functional provided by Perdew/Wang.[37] Aluminum, gallium, and indium atoms were represented by the relativistic effective core potential SDD (augmented by a *d* polarization function).[38] For the rest of the atoms the 6-31G(d,p) basis set was used.[39] Gibbs free energies were obtained at $T = 298.15$ K within the harmonic approximation. Intrinsic reaction paths[40] were followed from the various transition structures to verify the reactant-to-product linkage.

Acknowledgements

Y.S. and J.-F.C. warmly acknowledge financial support from Total Raffinage-Chimie (grant to N.M.). L.M. is grateful to CINES and CalMip (CNRS, Toulouse) for the grant of computing time.

Keywords: C–H activation · density functional calculations · gallium · hydride abstraction · indium · zwitterions

[1] a) K. R. Campos, *Chem. Soc. Rev.* **2007**, *36*, 1069; b) P. W. Roesky, *Angew. Chem.* **2009**, *121*, 4988; *Angew. Chem. Int. Ed.* **2009**, *48*, 4892.

[2] W. A. Nugent, D. W. Ovenall, S. J. Holmes, *Organometallics* **1983**, *2*, 161.

[3] a) S. B. Herzon, J. F. Hartwig, *J. Am. Chem. Soc.* **2007**, *129*, 6690; b) S. B. Herzon, J. F. Hartwig, *J. Am. Chem. Soc.* **2008**, *130*, 14940; c) P. Eisenberger, R. O. Ayinla, J. M. P. Lauzon, L. L. Schafer, *Angew. Chem.* **2009**, *121*, 8511; *Angew. Chem. Int. Ed.* **2009**, *48*, 8361; d) A. L. Reznichenko, K. C. Hultzsch, *J. Am. Chem. Soc.* **2012**, *134*, 3300.

[4] a) R. Kubiak, I. Prochnow, S. Doye, *Angew. Chem.* **2009**, *121*, 1173; *Angew. Chem. Int. Ed.* **2009**, *48*, 1153; b) J. A. Bexrud, P. Eisenberger, D. C. Leitch, P. R. Payne, L. L. Schafer, *J. Am. Chem. Soc.* **2009**, *131*, 2116; c) R. Kubiak, I. Prochnow, S. Doye, *Angew. Chem.* **2010**, *122*, 2683; *Angew. Chem. Int. Ed.* **2010**, *49*, 2626; d) I. Prochnow, P. Zark, T. Müller, S. Doye, *Angew. Chem.* **2011**, *123*, 6525; *Angew. Chem. Int. Ed.* **2011**, *50*, 6401.

[5] a) J. F. Hartwig, *J. Am. Chem. Soc.* **1996**, *118*, 7010; b) S. Sakaguchi, T. Kubo, Y. Ishii, *Angew. Chem.* **2001**, *113*, 2602; *Angew. Chem. Int. Ed.* **2001**, *40*, 2534; c) S. Doye, *Angew. Chem.* **2001**, *113*, 3455; *Angew. Chem. Int. Ed.* **2001**, *40*, 3351; d) K. Yamaguchi, N. Mizuno, *Angew. Chem.* **2003**, *115*, 1518; *Angew. Chem. Int. Ed.* **2003**, *42*, 1480; e) J. S. M. Samec, A. H. Éll, J. E. Bäckvall, *Chem. Eur. J.* **2005**, *11*, 2327; f) J. Cámpora, I. Matas, P. Palma, E. Alvarez, C. Graiff, A. Tiripicchio, *Organometallics* **2007**, *26*, 3840; g) M. Z. Wang, C. Y. Zhou, M. K. Wong, C. M. Che, *Chem. Eur. J.* **2010**, *16*, 5723.

[6] P. Horrillo-Martínez, K. C. Hultzsch, A. Gil, V. Branchadell, *Eur. J. Org. Chem.* **2007**, 3311.

[7] a) B. E. Bent, R. G. Nuzzo, L. H. Dubois, *J. Am. Chem. Soc.* **1989**, *111*, 1634; b) *Comprehensive Organometallic Chemistry II*, Volumes 1 and 11 (Eds.: E. W. Abel, F. G. A. Stone, G. Wilkinson), Elsevier Science Oxford, **1995**.

[8] a) K. Saito, Y. Shibata, M. Yamanaka, T. Akiyama, *J. Am. Chem. Soc.* **2013**, *135*, 11740; b) C. Zhu, T. Akiyama, *Adv. Synth. Catal.* **2010**, *352*, 1846.

[9] In nature, NADPH is a known reducing agent that switches to the coenzyme $NAPD^+$ (nicotinamide adenine dinucleotide phosphate) through formal loss of hydride in several biological processes; the transformation is driven by aromatization to a pyridinium moiety.

[10] a) W. Uhl, J. Grunenberg, A. Hepp, M. Matar, A. Vinogradov, *Angew. Chem.* **2006**, *118*, 4465; *Angew. Chem. Int. Ed.* **2006**, *45*, 4358; b) W. Uhl, A. Vinogradov, S. Grimme, *J. Am. Chem. Soc.* **2007**, *129*, 11259.

[11] a) E. L. Whitelaw, G. Loraine, M. F. Mahon, M. D. Jones, *Dalton Trans.* **2011**, *40*, 11469; b) Y. Wang, H. Ma, *Chem. Commun.* **2012**, *48*, 6729.

[12] Hydride abstraction with $[Ph_3C][B(C_6F_5)_4]$ in the ligand backbone of a bis(oxazolinato)gallium complex gave a cationic gallium species: S. Dagorne, S. Bellemin-Laponnaz, A. Maisse-François, M.-N. Rager, L. Jugé, R. Welter, *Eur. J. Inorg. Chem.* **2005**, 4206. For another similar example of hydride abstraction from a ligand backbone with $[Ph_3C][B(C_6F_5)_4]$ and generation of cationic zirconium complexes, see: B. Lian, L. Toupet, J.-F. Carpentier, *Chem. Eur. J.* **2004**, *10*, 4301 and references cited therein.

[13] Of interest, intramolecular C–H activation of *o*-*t*Bu groups in Mes*-substituted (Mes = mesityl) phosphaalkene–MCl_3 (M = Al, Ga, In) adducts leads to coordinated ylide–MCl_3 zwitterions: C.-W. Tsang, C. A. Rohrick, T. S. Saini, B. O. Patrick, D. P. Gates, *Organometallics* **2004**, *23*, 5913.

[14] a) W. Petz, C. Kutschera, S. Tschan, F. Weller, B. Neumüller, *Z. Anorg. Allg. Chem.* **2003**, *629*, 1235; b) F. Molinos de Andrade, W. Massa, C. Peppe, W. Uhl, *J. Organomet. Chem.* **2005**, *690*, 1294.

[15] a) M. Sircoglou, M. Mercy, N. Saffon, Y. Coppel, G. Bouhadir, L. Maron, D. Bourissou, *Angew. Chem.* **2009**, *121*, 3506; *Angew. Chem. Int. Ed.* **2009**, *48*, 3454; b) E. J. Derrah, M. Sircoglou, M. Mercy, S. Ladeira, G. Bouhadir, K. Miqueu, L. Maron, D. Bourissou, *Organometallics* **2011**, *30*, 657.

[16] See the Supporting Information for details.

[17] This is further corroborated by the fact that the formation of an indium zwitterion also seems to occur if phenyl is replaced by an anthracenyl (anth) substituent on the pyrimidine heterocycle in $\{ON^{\wedge}(CH(anth))^{\wedge}NO\}H_2$ (the resulting compound could not be adequately characterized owing to its very poor solubility), whereas no zwitterion whatsoever could be synthesized with the very hindered $\{^{tBu2}ON^{\wedge}(CH_2)^{\wedge}NO^{tBu2}\}H_2$ proteo-ligand bearing *t*Bu substituents in *ortho* and *para* positions of the phenolic rings (see the Supporting Information). Attempts to obtain $\{ON^{\wedge}(CH(CF_3))^{\wedge}NO\}H_2$, $\{ON^{\wedge}(CH(tBu))^{\wedge}NO\}H_2$, and $\{ON^{\wedge}(CH(mes))^{\wedge}NO\}H_2$ (mes = mesityl) were unsuccessful, thus precluding the further evaluation of electronic and steric considerations.

[18] The distances from N(19) to the two Al atoms of 3.66 and 4.65 Å rule out coordination to the metal centers.

[19] For leading reviews on Al–salen complexes, see: a) D. A. Atwood, M. J. Harvey, *Chem. Rev.* **2001**, *101*, 37; b) S. Bellemin-Laponnaz, S. Dagorne, 'Coordination chemistry and applications of salen, salan and salalen metal complexes', in *The Chemistry of Metal Phenolates* (Ed. Zabicky, J.), John Wiley & Sons, Ltd, Chichester, **2012**.

[20] P. Hormnirun, E. L. Marshall, V. C. Gibson, A. J. P. White, D. J. Williams, *J. Am. Chem. Soc.* **2004**, *126*, 2688.

[21] N. C. Johnstone, E. S. Aazam, P. B. Hitchcock, J. R. Fulton, *J. Organomet. Chem.* **2010**, *695*, 170.

[22] a) I. Peckermann, A. Kapelski, T. P. Spaniol, J. Okuda, *Inorg. Chem.* **2009**, *48*, 5526; b) I. Yu, A. Acosta-Ramírez, P. Mehrkhodavandi, *J. Am. Chem. Soc.* **2012**, *134*, 12758; c) D. C. Aluthge, B. O. Patrick, P. Mehrkhodavandi, *Chem. Commun.* **2013**, *49*, 4295.

[23] For the description of a related pyrimidinium core, see: T. W. Hudnall, C. W. Bielawski, *J. Am. Chem. Soc.* **2009**, *131*, 16039.

[24] G. R. Fulmer, A. J. M. Miller, N. H. Sherden, H. E. Gottlieb, A. Nudelman, B. M. Stoltz, J. E. Bercaw, K. I. Goldberg, *Organometallics* **2010**, *29*, 2176.

[25] The precursor $\{^{Me}ON^{\wedge}(CH_2)^{\wedge}NO^{Me}\}Li_2$ required to prepare $\{^{Me}ON^{\wedge}(CH_2)^{\wedge}NO^{Me}\}D_2$ and, from here, **7-D**, crystallized as the tetrametallic complex $[\{ON^{\wedge}(CH_2)^{\wedge}NO\}Li{\cdot}Li(THF)_2]_2$ from THF. The four four-coordinated Li atoms present an unusual linear arrangement; see the Supporting Information for details.

[26] The formation of **6** is slow, and requires a long reaction time at high temperature; it is very likely that **6** and **8-H**, which need not be present in large amounts, are in the presence of each other at some stage of the reaction, and react with one another to yield **9**.

[27] M. Sircoglou, N. Saffon, K. Miqueu, G. Bouhadir, D. Bourissou, *Organometallics* **2013**, *32*, 6780.

[28] D. W. Stephan, G. Erker, *Angew. Chem.* **2010**, *122*, 50; *Angew. Chem. Int. Ed.* **2010**, *49*, 46 and references therein.

[29] A. M. Chapman, M. F. Haddow, D. F. Wass, *J. Am. Chem. Soc.* **2011**, *133*, 18463.

[30] C. Appelt, H. Westenberg, F. Bertini, A. W. Ehlers, J. C. Slootweg, K. Lammertsma, W. Uhl, *Angew. Chem.* **2011**, *123*, 4011; *Angew. Chem. Int. Ed.* **2011**, *50*, 3925.

[31] *The Group 13 Metals Aluminium, Gallium, Indium and Thallium: Chemical Patterns and Peculiarities* (Eds: S. Aldridge, A. J. Downs), Wiley, Hoboken, **2011**.

[32] Attempts to deprotonate the pentahydropyrimidinium moiety (by treatment of **3** with potassium bis(trimethylsilyl)amide (KHMDS) or other strong bases) to access the corresponding NHC carbene species were unsuccessful.

[33] a) O. T. Beachley Jr., R. N. Rusinko, *Inorg. Chem.* **1979**, *18*, 1966; b) O. T. Beachley Jr., R. G. Simmons, *Inorg. Chem.* **1980**, *19*, 1021.

[34] a) G. M. Sheldrick, SHELXS-97, *Program for the Determination of Crystal Structures*; University of Goettingen: Germany, **1997**; b) G. M. Sheldrick, SHELXL-97, *Program for the Refinement of Crystal Structures*; University of Goettingen: Germany, **1997**.

[35] Gaussian 09, Revision A.02, M. J. Frisch, G. W. Trucks, H. B. Schlegel, G. E. Scuseria, M. A. Robb, J. R. Cheeseman, G. Scalmani, V. Barone, B. Mennucci, G. A. Petersson, H. Nakatsuji, M. Caricato, X. Li, H. P. Hratchian, A. F. Izmaylov, J. Bloino, G. Zheng, J. L. Sonnenberg, M. Hada, M. Ehara, K. Toyota, R. Fukuda, J. Hasegawa, M. Ishida, T. Nakajima, Y. Honda, O. Kitao, H. Nakai, T. Vreven, J. A. Montgomery, Jr., J. E. Peralta, F. Ogliaro, M. Bearpark, J. J. Heyd, E. Brothers, K. N. Kudin, V. N. Staroverov, R. Kobayashi, J. Normand, K. Raghavachari, A. Rendell, J. C. Burant, S. S. Iyengar, J. Tomasi, M. Cossi, N. Rega, J. M. Millam, M. Klene, J. E. Knox, J. B. Cross, V. Bakken, C. Adamo, J. Jaramillo, R. Gomperts, R. E. Stratmann, O. Yazyev, A. J. Austin, R. Cammi, C. Pomelli, J. W. Ochterski, R. L. Martin, K. Morokuma, V. G. Zakrzewski, G. A. Voth, P. Salvador, J. J. Dannenberg, S. Dapprich, A. D. Daniels, O. Farkas, J. B. Foresman, J. V. Ortiz, J. Cioslowski, D. J. Fox, Gaussian, Inc., Wallingford CT, **2009**.

[36] A. D. Becke, *J. Chem. Phys.* **1993**, *98*, 5648.

[37] J. P. Perdew, Y. Wang, *Phys. Rev. B* **1992**, *45*, 13244.

[38] a) A. Bergner, M. Dolg, W. Kuchle, H. Stoll, H. Preuss, *Mol. Phys.* **1993**, *80*, 1431; b) T. Leininger, A. Berning, A. Nicklass, H. Stoll, H.-J. Werner, H.-J. Flad, *Chem. Phys.* **1997**, *217*, 19.

[39] a) R. Ditchfield, W. J. Hehre, J. A. Pople, *J. Chem. Phys.* **1971**, *54*, 724; b) W. J. Hehre, R. Ditchfield, J. A. Pople, *J. Chem. Phys.* **1972**, *56*, 2257; c) P. C. Hariharan, J. A. Pople, *Theor. Chim. Acta.* **1973**, *28*, 213.

[40] a) C. Gonzalez, H. B. Schlegel, *J. Chem. Phys.* **1989**, *90*, 2154; b) C. Gonzalez, H. B. Schlegel, *J. Phys. Chem.* **1990**, *94*, 5523.

Received: February 26, 2014
Published online on May 19, 2014